ISSN 0006-3509, Biophysics, 2008, Vol. 53, No. 3, pp. 237–242. © Pleiades Publishing, Inc., 2008.
Original Russian Text © V.A. Ryabov, 2008, published in Biofizika, 2008, Vol. 53, No. 3, pp. 504–512.

COMPLEX SYSTEMS
BIOPHYSICS

Acoustic Clutter Field and Echo Reception by the Dolphin

V. A. Ryabov

Karadag Natural Reserve, National Academy of Sciences of Ukraine, Kurortnoe, Crimea, 98188 Ukraine
E-mail: ryaboff@ukr.net

Received February 15, 2007; in final form, October 18, 2007

Abstract—A model is considered for an acoustic field of echolocation-hampering reflections (clutter) from steel cylinders; its analysis reveals vast possibilities of improving the signal-to-noise ratio through clutter interference. Current models of dolphin hearing are collated with the acoustic clutter field. It is most likely that the lower jaw (mental) foramens take part in echo conduction to the cochlea. In this case the receiver aperture is determined by the size of the foramens, and the receiver base is the distance between them in the jaw halves; the adequacy of these parameters to the clutter field can substantially protect the echo reception in odontocetes against reverberation.

Key words: odontocetes, hearing, echolocation, mental foramens, signal-to-clutter ratio

DOI: 10.1134/S0006350908030123

INTRODUCTION

Echolocation and hearing in toothed whales (Odontoceti) and particularly dolphins has been the subject of numerous works. There is, however, no unanimity about the pathways of echo conduction to the inner ear. Two ways are mainly considered. One way is via the external auditory meatus [1] or through the soft tissues of the head to the proximal portion of auditory passage [2, 3] and the middle ear. Some authors think that auditory passages are not involved at all [4–6] or conduct only low-frequency signals [7–9]. There may be two functionally specialized subsystems of passive (1–10 kHz) and active (~100 kHz) hearing [10]. The second way involves the fat body of the lower jaw and the tympanic bone, bypassing the external auditory passages and the tympanic ligament [5, 8, 11–15]. The echoes enter the fat body through the anterior (mental) foramens [11] or directly through the bone at the "acoustic window" [12, 14], pass to the tympanic plate and then to the malleus [11–17]. Low-frequency sounds and communication signals in this case may reach the middle ear via the external fat funnel overlaying the pan bone [14].

Some echolocation experiments favor the second pathway. Acoustic shielding of the lower jaw markedly impaired the dolphin's performance [18]. The bottlenose dolphin is thought to use the 40–140 kHz range for echolocation [19, 20]; the spectral maximum of its sounding pulse energy coincides with the intervals of maximal sensitivity (110–120 kHz) [21, 22] and minimal differentiation thresholds [19, 23]. Such functional correspondence is observed for other dolphins as well [24–26].

Acoustic stimulation of the lower jaw was also shown to cause significant evoked potentials in the dolphin's central auditory system [5, 8]. However, the regions of maximal sensitivity of the lower jaw surface to sounds from contact point emitters vary in different works [5, 8, 27–29], and the results do not explain the conduction mechanism.

Also discussed is the possibility of concurrent involvement of the external acoustic passages and the "acoustic windows" in feeding the sound to the cochlea to create a spatial auditory image [30].

Modeling of target echolocation [31, 32] gives additional grounds for regarding the mental foramens as acoustic channels to the mandibular fat body. Therewith the right and the left halves of the lower jaw are considered as traveling wave antennas [33–37].

Which of the conduction models is most consistent with echolocation hearing? Dolphins are known to perform well in locating targets under conditions of reverberation, and their hearing is highly adapted to extraneous reflections (clutter). Reverberation is an overall echo signal caused by reflections of the emitted sounding pulse from objects and inhomogeneities of the medium; its intensity is proportional to that of the emitted pulse, so the signal/clutter ratio would not be reduced by merely changing the pulse level. Therefore, dolphin's hearing must be somehow conciliated with the acoustic clutter field. With such premises, the goal of the present work was to assess this putative adequacy by (i) constructing and examining a model of the clutter field, (ii) looking for possible means to reduce its influence, and (iii) collating this model with echo conduction models.

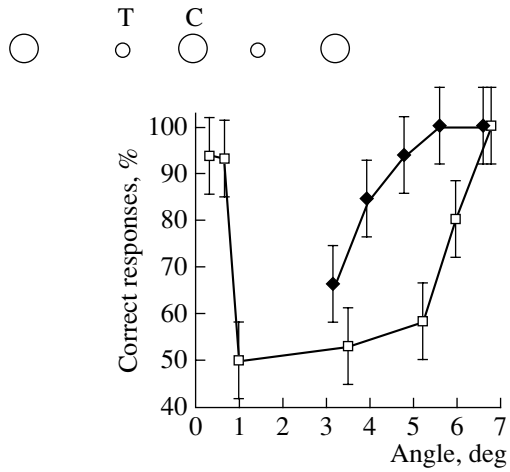

Fig. 1. Discrimination of targets (T) by an echolocating dolphin as dependent on the angle between two outward cylinders relative to the separating net [31] (because of symmetry, the right half-plane is considered in the plot) and the effect of adding a third central cylinder (C): empty squares for two cylinders, filled rhombi for three.

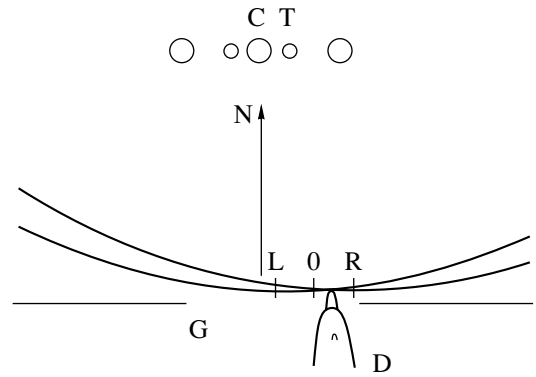

Fig. 2. Outlay of the experiment [31] (viewed from above): N, separating net; G, start gate; D, dolphin's head; L0R, the region modeled for the echo from the central and right cylinders with intersecting wavefronts; C, cylinder (steel, 6 cm diameter, 13 cm high); T, target spheres (brass, 5 (positive) and 3 cm diameter) separated ±1.4° relative to the net at the start; distance from start to T/C, 7.5 m; spheres, cylinders, and start at a depth of 1 m.

EXPERIMENTAL DATA

Use was made of the data on target (brass spheres) discrimination by the dolphin in acoustic clutter from steel cylinders [31]. It has been established that the dolphin compares the targets in every trial, and fails to distinguish them if one target is masked. Cylinders placed between the targets (angles less than ±1.4°) cause no hindrance as long as the angular T–C distance exceeds 0.5° (Fig. 1). In this case the high T/C discrimination is explained by the directionality of dolphin's emission and reception. As the steepness of the complete (emission–hearing) directionality characteristic (DC) reaches 5 dB/deg and rises away from the maximum, the DC slopes are used to attenuate the extraneous echoes. Thus for angular location of the (left or right) target the dolphin can "orientate the DC" so that the T and C echoes fall on one (right or left) slope. When the cylinders are outward to the targets (angles more than ±1.4°) the dolphin has to use both DC slopes, and the threshold T–C distance increases by an order of magnitude [31].

To complicate the problem, a third cylinder was added between the targets (Fig. 1); most intriguingly, it turned out that the discrimination of spheres was less hindered by three cylinders than by two or even one. Thus the dolphin failed with two cylinders at an angle less than ±6°, but with the third cylinder in the middle the dolphin performed confidently down to ±3.5° (rhombi). The hindrance from three cylinders of 6-cm diameter was found to be equivalent to that from two outward cylinders of 0.6 cm. To understand this effect, consider the configuration of the experiment (Fig. 2). The angular distance between cylinders as seen from the start position was chosen to be less than the width of the emission DC. In this case the dolphin can register only two cylinders simultaneously (central and either of the side ones). The incoming reflections from the cylinders are coherent, as echo of one sounding pulse. Hence it can be supposed that the dolphin uses the interference between reflections from the two cylinders, whereby their influence is attenuated. To test this suggestion, a model was built for the cylinder echo field in the area of the start position (LØR, Fig. 2).

MODEL

Digitized echo signals were obtained upon exposing a cylinder to pulses resembling those used by the dolphin in echolocation [19] (Fig. 3a). Two such signals, from the central and the right cylinders in Fig. 2, were use to simulate the profiles of the acoustic clutter field. Each profile is a superposition of echoes (Fig. 3) with delays corresponding to its position in the L0R area.

The central profile (0 cm in Fig. 4) is calculated for equal distances (7.5 m) to the cylinders. All profiles are stored as an Excel-type electronic table. This data relation model displays the distribution of the relative sound pressure of echoes at L0R in 1-cm steps as a 3D surface composed of 81 profiles.

The "far zone" where the phase difference between plane and spherical wavefronts becomes small enough is determined from $r = L^2/\lambda$; hence the span of the spherical wavefront reaching the start area (r = 7.5 m) that can be approximated with a plane wave is $L = \sqrt{r\lambda}$ = 33 cm (r = 7.5 m, $\lambda \approx 1.4$ cm is the wavelength of energy maximum). The phase difference at the edges of this span (±16.5 cm from the center) would be $<\lambda/8$ (Figs. 4–6). In simulation profiles for larger distances from the center, there is no interference of the cylinder echoes (Figs. 4–6). Note that at the characteristic points the field parameters were recalculated in the piecewise-

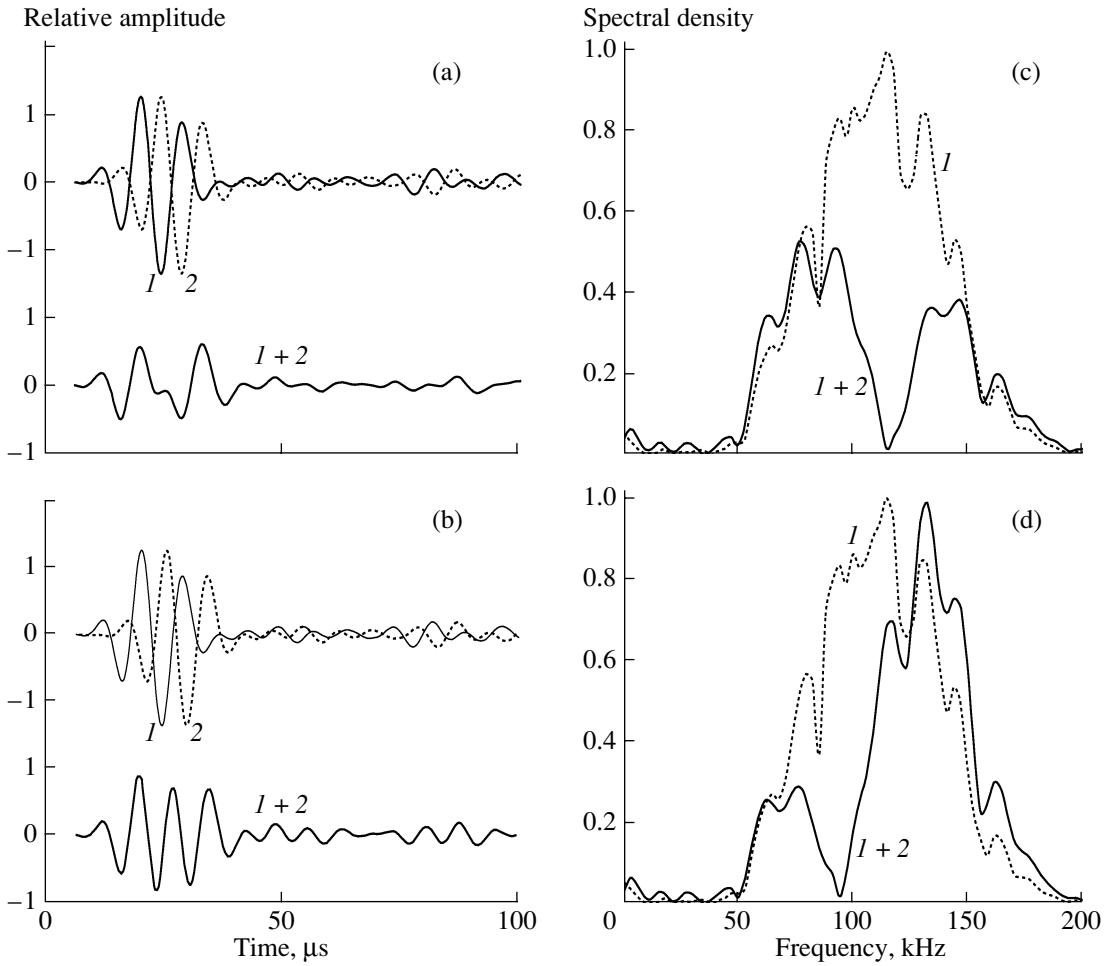

Fig. 3. (a, b) Echo of the right (*1*) and the central cylinder (*2*) delayed by (a) 4.33 and (b) 5.33 μs; (*1* + 2) their superpositions corresponding to profiles (a) ±6.5 and (b) 8 cm; (c, d) the corresponding energy spectra.

linear approximation of a spherical field, without basic differences from the plane wave approximation.

RESULTS

In Fig. 4 one can see the typical echo interference pattern. As the wave velocities are the same, the pattern propagates in the direction of the acoustic profiles. Along the same direction one can see regions with low amplitudes throughout. For more detailed analysis, consider the model surface in the plane normal to the direction of propagation (Fig. 5). In this section the model reproduces the distribution of the maximal relative pressure of cylinder echoes, P_m. The width of the minima (more than 6 dB mutual attenuation) does not exceed 3 cm. The clutter energy flux density in each profile is calculated as

$$E = \frac{1}{\rho c}\int_0^\infty P^2(t)dt,$$

where $P(t)$ is the time dynamics of sound pressure.

The distribution of relative energy fluxes (Fig. 6) generally corresponds to that of maximal amplitudes, also with two profound minima. At 2–3 cm width, the energy cancellation factor is 4–6. In the general case the width of the minima depends on the angular distance between the cylinders, increasing monotonously from 6

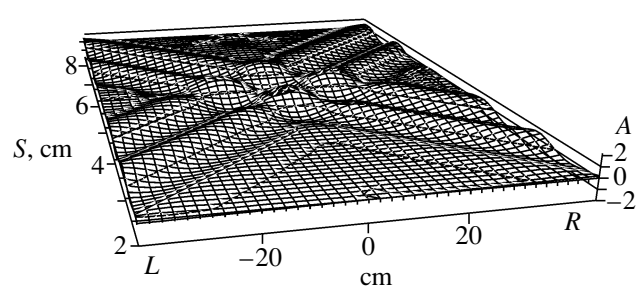

Fig. 4. Simulated field of echo from the cylinders. *L0R*, horizontal distribution of sound pressure profiles; *S*, length of pressure profiles in the direction of propagation of the interference pattern; *A*, relative amplitude of sound pressure.

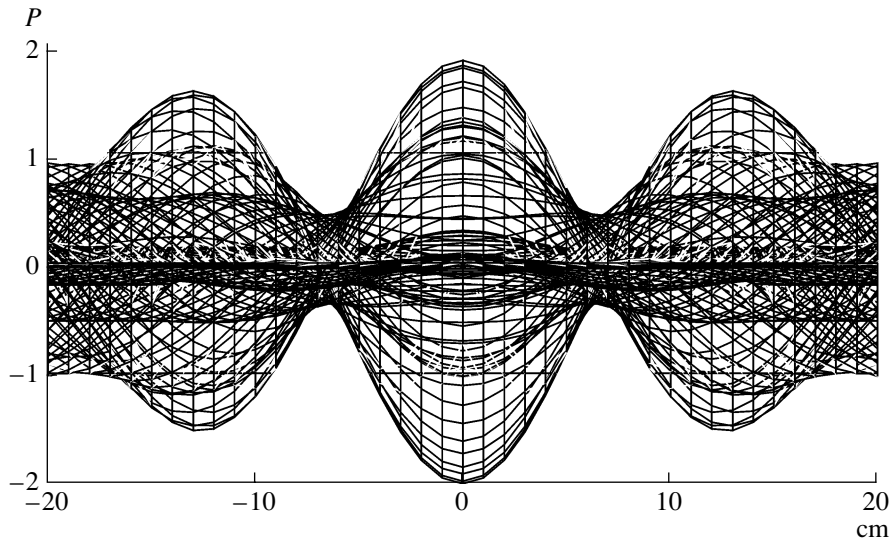

Fig. 5. Distribution of maximal relative amplitudes of sound pressure in the simulated profiles. Beyond the interference zone, P_m = const = P_1. Angle between cylinders, ±6°.

to 11 cm (at level 1) with angular variation from ±6.5 to ±3.5°; therewith the distance between the minima increases from 13 to 24 cm. The expanse of the interference region S (Fig. 4) is determined by the duration of clutter reflections (~30 μs) and at sound velocity in water C = 1500 m/s it is $S = Ct$ = 4.5 cm. The energy spectra of the superposition of echoes differ essentially for particular profiles, as exemplified in Fig. 3; the frequency F_0 where the clutter is attenuated most profoundly (tens of times) changes from 62.5 to 150 kHz in the profiles from ±12 to ±5 cm with delays of 8 to 3.33 μs.

DISCUSSION

In the central profile of the model (0 cm) the clutter echoes sum up without delay (Figs. 4–6) to give the highest amplitude and energy. Away from the center, an increasing delay appears between the echoes. In the ±6.5 cm (Fig. 5) and ±12 cm (Fig. 6) profiles the delay reaches half the echo period, which corresponds to the main interference minima. Analysis of the model shows that the best conditions for cancellation are the equality of amplitudes and a half-period delay (~5 μs); thereby the maximal amplitude decreases by a factor of 2.5 (7.6 dB, Fig. 5) and the sum energy drops 7 times (8.5 dB, Fig. 6).

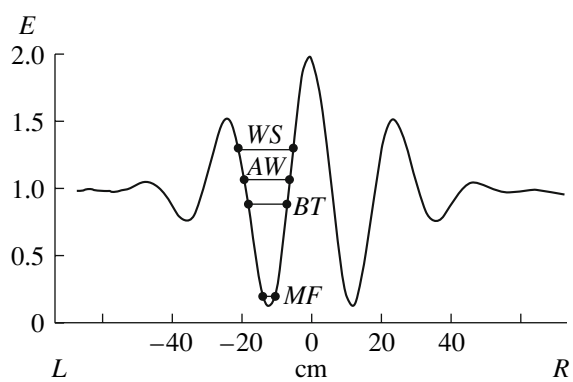

Fig. 6. Distribution of relative clutter energy flux density in the simulated profiles. Beyond the interference zone, E = const = E_1. Angle between cylinders, ±3.5°. *MF*, maximal distance between mental foramens of the lower jaw halves (3.5 cm); *BT*, distance between tympanic bullae (12 cm); *AW*, distance between "acoustic windows" (13.5 cm); *WS*, skull width at external meatuses (16.5 cm).

Still more dramatic is the picture in the spectrum (Fig. 3): at the energy maximum (F_0 = 114.3 kHz), i.e., in the region of maximal hearing sensitivity [21, 22], the clutter from two cylinders is suppressed 59 times (17.7 dB) as compared with the echo from a single cylinder.

The frequency at which clutter is maximally suppressed changes monotonously from profile to profile and, in accordance with theory, is determined by the frequency-axis position of the first zero in the modulus of the envelope energy spectrum of a pulse pair as a function of the time delay: $F_0 = 1/2t_d$. The fact that in the model the amplitudes at F_0 are nonzero is caused by the finite value of signal discretization.

Thus, we see that there are vast possibilities for attenuating acoustic clutter by interference. So what characteristics a receiver must have to take advantage of these options? Let us look at Figs. 5 and 6. It is easy to see that spatial resolution of the model surface to an accuracy of changes in each profile is possible if the receiver has an aperture smaller than the distance between profiles. This is also favored by the fact that the interference pattern propagates along the direction to the target(s), and a receiver with a small enough aperture (less than the width of the interference minimum)

can stay in the area of the minimum throughout the clutter. In this case the signal/clutter ratio rises proportionally to the clutter suppression. For the resolution of the receiver to be the same in the horizontal and vertical planes, the shape of the aperture should be close to a circle. However, the diameter of the aperture (D) should not be too small, as this would perhaps limit the transmitted energy and thereby lower the sensitivity.

The restriction on the aperture D, by analogy to the slit used in magnetic and transverse optical recording, can be written as $D \leq \Delta/2$ where Δ is the minimal distance between analyzed profiles of the field (in the model, $\Delta = 1$ cm and $D \leq 0.5$ cm). By the same reasoning, for a nondirectional receiver D is limited by the wavelength of the highest perceptible frequency (for $F_0 = 150$ kHz, $\Delta = \lambda = 1$ cm and $D = \lambda/2 \leq 0.5$ cm).

A receiver with the above features, which will be called the optimal-aperture receiver (OAR), can use all the above possibilities of improving the signal/clutter ratio. One such receiver, if moved in an acoustic field with repeated sounding, allows a broadband echo signal at the background of clutter with interfering spectral components to be analyzed consecutively throughout the frequency range.

Furthering this idea, multichannel reception with a series of D-spaced OARs and analysis of their inputs by narrow bands (overlapping the target echo band) would perhaps provide the same signal/clutter improvement simultaneously over the entire frequency band (time-parallel at single sounding) by summation of the best-ratio channels.

An important issue from the field simulation concerns binaural hearing: to gain fully and most simply from clutter interference, the distance between two OARs should fit into the width of one interference minimum. Otherwise the reception may improve in one "channel" but would most probably deteriorate in the other. As evident from Fig. 6, the only paired elements related to dolphin's hearing that meet the above conditions are the mental foramens.

Thus, there are grounds for supposing that the echo signals are conducted through the pathway comprising the mental foramens, mandibular fat body, and middle ear, with matched water/ear impedance in the echolocation range 40–140 kHz [37] and optimal DC [36], and probably with the best signal/clutter ratio, as the size of the foramens (aperture, ~0.3 cm) and the spacing between them (receiver base, 0.75–3.5 cm) are consistent with the widths of clutter interference minima. All this can serve to protect the dolphin's sonar against reverberation.

The conclusions from model analysis are supported by the behavior of the dolphin at the start in the sphere discrimination task (Fig. 2). The animal repeatedly probed the targets during slow head movements, probably searching for optimal directions of the emitter and receiver relative to targets and decoys. Notably, if the central cylinder was moved more than 8 cm ahead or behind the target plane (i.e., closer to or farther from the dolphin), the interference region shifted away from the start area, and in this case the third cylinder did not alleviate the task [31].

In adaptation to aquatic life, odontocetes experienced extensive modifications of the skull. It is tempting to think that the most vivid feature known as telescoping [38] was, among other reasons, associated with the development of the peripheral part of echolocation hearing in the lower jaw, while the convergence of the jaw halves at the level of mental foramens reflects the optimization of the receiver aperture and base.

REFERENCES

1. F. C. Fraser and P. E. Purves, Bull. Brit. Museum Nat. History, Zool. **7** (1), 1 (1960).
2. F. W. Reysenbach de Haan, Acta Otolaryngol. Suppl. **134**, 1 (1956).
3. W. H. Dudok van Heel, Neth. J. Sea. Res. **1**, 407 (1962).
4. M. Yamada, Contribution to the anatomy of the organ of hearing of whales. Sci. Rep. Whales. Res. Inst. **8**, 1 (1953).
5. J. G. McCormick, E. G. Wever, J. Palin, and S. H. Ridgway, J. Acoust. Soc. Amer. **48** (6), 1418 (1970).
6. G. Fleischer, J. Audit. Res. **13**, 178 (1973).
7. E. Sh. Airapetiants, V. A. Voronov, Yu. V. Ivanenko, et al., Zh. Evol. Biokhim. Fiziol. No. 2, 418 (1973).
8. T. H. Bullock, A. D. Grinell, E. Ikezono, et al., Z. Vergl. Physiol. **59**, 117 (1968).
9. D. L. Renaud and A. N. Popper, J. Exp. Biol. **63**, 569J (1975).
10. N. A. Dubrovsky, in Sensory Abilities of Cetacean, Ed. by J. Thomas, R. Kastelein (Plenum Press, N.Y., 1990), pp. 233-254.
11. K. S. Norris, in *Marine Bio-Acoustics*, Ed. by W. Tavolga (Pergamon Press, N.Y., 1964), pp. 316–336.
12. K. S. Norris, in *Evolution and Environment*, Ed. E. Drake (Yale Univ. Press, N. Haven, 1968), pp. 297–324.
13. K. S. Norris and G. W. Harvey, J. Acoust. Soc. Amer. **56** (2), 659 (1974).
14. D. R. Ketten, Intern. J. Anim. Sound and Rec. **8**, 103 (1997).
15. H. N. Koopman, S. M. Budge, D. R. Ketten, and S. J. Iverson, J. Ocean. Engin. **31** (1), 95 (2006).
16. S. Nummela, T. Reuter, S. Hemila, et al., Hear. Res. **133** (1–2), 61 (1999).
17. S. Hemila, S. Nummela, and T. Reuter, Hear. Res. **133**, 82 (1999).
18. R. L. Brill, in *Animal Sonar*, Ed. by P. Nachtigall, P. Moor (Plenum Press, N.Y., 1988), pp. 281-287.
19. V. A. Ryabov, Candidate's Dissertation in Biology (St. Petersburg, 1991).
20. V. A. Ryabov and G. L. Zaslavskii, Sensornye Sistemy **12** (2), 202 (1998).
21. V. I. Chilingiris, *Abstr. 9th Acoust. Conf.* (Moscow, 1977), Sect. C., pp. 17–20.
22. E. S. Babushina, Biofizika **45**, 927 (2000).

23. E. S. Babushina and M. A. Polyakov, Biofizika **48**, 332 (2003).

24. W. W. L. Au, in *Animal Sonar Systems,* Ed. by R. Busnel, J. Fish (Plenum Press, 1980), pp. 251–282.

25. W. A. Watkins and D. Wartzok, Mar. Mamm. Sci. **1**, 219 (1985).

26. N. G. Bibikov, in *Marine Mammal Sensory Systems*, Ed. by J. Thomas, R. Kastelein, A. Supin (Plenum press, N.Y., 1992), pp. 197-211.

27. B. Mehl, W. W. L. Au, J. Pawloski, and P. E. Nachtigall, J. Acoust. Soc. Amer. **105**, 3421 (1999).

28. R. L. Brill, P. W. B. Moor, and L. A. Dankiewicz, J. Acoust. Soc. Amer. **109**, 1717 (2001).

29. R. L. Brill, P. W. B. Moore, D. A. Helweg, and L. A. Dankiewicz, Technical report no. 1865, 1 (2001).

30. L. K. Rimskaya-Korsakova and N. A. Dubrovskii, Sensornye Sistemy **12** (4), 497 (1998).

31. V. A. Ryabov and G. L. Zaslavskii, Sensornye Sistemy **13** (4), 337 (1999).

32. V. A. Ryabov, http://edok01.tib.uni-hannover.de/edoks/e01mr01/367010372.pdf 2002.

33. V. A. Ryabov, http://edok01.tib.uni-hannover.de/edoks/e01mr01/367007592.pdf 2003.

34. V. A. Ryabov, in *Abstracts of the XlXth meeting of IBAC*. www.cultura.uipa.br/ibac 2003.

35. V. A. Ryabov, J. Acoust. Soc. Amer. **114** (4), 2414 (2003).

36. V. A. Ryabov, in *Marine Mammals of the Holarctic*, Ed. V. Belcovich (KMK Scientific Press, Moscow, 2004), pp. 483–489.

37. V. A. Ryabov, in *Fourth Int. Conf. on BioAcoustics, Loughborough University, UK.*, Ed. by S. Dible, P. Dobbins, J. Flint, E. Harland, P. Lepper (Proceedings of the Institute of Acoustics, 2007). Vol. 29, Pt. 3, pp. 283–293.

38. G. S. Miller, The telescoping of the cetacean skull. Smithsonian Misc. Coll.. Vol. 76, pp. 1-67 (1923).